Adsorption and thermal decomposition of acetic acid on Si(111)7×7 studied by vibrational electron energy loss spectroscopy

V. Venugopal, A. Chatterjee, M. Ebrahimi,[a] Z. H. He, and K. T. Leung[b]
Department of Chemistry and WATLab, University of Waterloo, Waterloo, Ontario N2L 3G1, Canada

(Received 14 February 2010; accepted 29 March 2010; published online 3 May 2010)

Vibrational electron energy loss spectroscopy (EELS) has been used to characterize the adsorption of acetic acid on Si(111)7×7 at room temperature and as a function of annealing temperature. At room temperature, acetic acid is found to undergo O—H dissociative adsorption to form predominantly unidentate adstructure. The equilibrium geometry and the corresponding characteristic vibrational wavenumbers of the adstructures were obtained by density functional theory calculations and are found to be in good accord with the vibrational EELS data. Annealing the sample near 473 K marked the onset of C—O dissociation of the acetate adstructure with the emergence of Si—O—Si vibrational modes at 720 and 1020 cm^{-1}. Further annealing to 673 K caused a marked intensity reduction in the C—C stretch at 930 cm^{-1} and in the CH_3 vibrational features at 1360 and 2990 cm^{-1}, suggesting further dissociation of the adstructures. The complete removal of the blueshifted Si—H stretching mode at 2275 cm^{-1} upon further annealing to 773 K is consistent with the recombinative desorption of H_2 from Si monohydrides expected in this temperature range. The emergence of the Si—C stretching mode at 830 cm^{-1} at 873 K is in good accord with the formation of SiC. Similar thermal evolution of the vibrational features have also been observed for acetic acid adsorption on a sputtered Si(111) surface. © *2010 American Institute of Physics*. [doi:10.1063/1.3400647]

I. INTRODUCTION

Adsorption of organic molecules on a silicon surface has continued to attract a lot of attention due to potential applications in nonlinear optics, biological sensors,[1] and molecular electronics.[2] Understanding the surface reactions of organic molecules driven thermally or by light and/or electron irradiation is essential for organic functionalization of the silicon surface, a common precursor step in application development. Together with amine and alcohol, carboxylic acid plays a particularly important role in biological surface science and in biofunctionalization of a semiconductor surface in particular,[3–6] which is practically relevant to bioelectronics.[7] As one of the small molecules with a carboxyl group [with formic acid (HCOOH) being the simplest], acetic acid (CH_3COOH), and its adsorption and surface chemistry on a semiconductor surface has been the subject of several recent investigations. In particular, our group has recently studied the room-temperature adsorption and thermal chemistry of acetic acid on Si(100)2×1 by using x-ray photoelectron spectroscopy (XPS) and density functional theory (DFT) calculations.[8] Acetic acid was found to adsorb on the 2×1 surface through O—H dissociation, producing both bidentate acetate at a lower exposure and unidentate acetate at a higher exposure.[8] Lee *et al.*[9] also recently investigated the room-temperature adsorption of acetic acid on Si(100)2×1 by using XPS and near-edge x-ray absorption fine structure but reported only the unidentate acetate adstructure. Earlier, Kim and Cho[10] had investigated reaction pathways of acetic acid on Si(100) by DFT calculations and predicted that the preferred mode of adsorption at room temperature is via O—H dissociation, as was later verified by Lee *et al.*[9] and also by our recent work.[8] Using DFT calculations, Carbone and Caminiti[11] obtained two fragmentation pathways of acetic acid on Si(100)2×1 involving Si—O—Si structure and C—C bond cleavage. Reaction pathways of acetic acid on Ge(100)2×1 resulting in unidentate, end-bridge bidentate and on-top bidentate adstructures were also studied by Kim and Cho[12] by using DFT calculations. Using scanning tunneling microscopy, Hwang *et al.*[13] observed the aforementioned bidentate acetate adstructures on the Ge(100)2×1 surface and the conversion of end-bridge to on-top bidentate adstructure upon annealing. In a combined XPS, Fourier transform infrared spectroscopy and DFT study, Filler *et al.*[14] reported chemisorption of acetic acid on Ge(100)2×1 at 310 K via O—H dissociation, producing unidentate acetate adspecies, with the likely additional formation of bridge-bidentate acetate adspecies at a lower coverage, similar to our recent result found for acetic acid on Si(100)2×1.[8] Adsorption of acetic acid on Ge(100) has been studied by Kim *et al.*[15] using DFT calculations, which also confirmed the bridge-bidentate adstructure to be energetically most favorable.

In contrast to the Si(100)2×1 surface, on which each surface Si atom offers two dangling bonds for surface reactions, the Si(111)7×7 surface offers a different reaction environment with a single dangling bond for each surface Si atom. In the dimer-adatom-stacking fault model of Takay-

[a]Present address: Department of Chemistry, University of Toronto, 80 St. George Street, Toronto, Ontario M5S 3H6, Canada.
[b]Author to whom correspondence should be addressed. Electronic mail: tong@uwaterloo.ca.

anagi *et al.*,[16] the Si(111)7×7 surface is represented by a unit cell containing 19 dangling bonds distributed over 12 adatom, 6 restatom, and 1 corner-hole atom sites. To date, no study has been reported for acetic acid on Si(111)7×7. Of the considerable limited amount of work on carboxylic acids on the 7×7 surface, adsorption of carboxylic acids such as formic acid (HCOOH)[17,18] and methacrylic acid (CH_2═CCH_3COOH) (Ref. 19) on Si(111)7×7 has been found to result in O—H bond cleavage, forming unidentate carboxylate adspecies. This type of O—H dissociative adsorption has been driven by the electron-deficient adatoms and the electron-rich restatoms on the Si(111)7×7 surface, which act as electron acceptors for the unidentate acetate and electron donors for the dissociated H atoms, respectively. In the present work, we investigate the adsorption of acetic acid on Si(111)7×7 as deposited at room temperature and as a function of annealing temperature by vibrational electron energy loss spectroscopy (EELS). DFT calculations are also used to determine the plausible adstructures and to compare the corresponding calculated vibrational wavenumbers with the experimental EELS data. We also compare the data with those obtained for adsorption of acetic acid on a sputtered Si(111)7×7 surface to examine the effect of surface conditions.

II. EXPERIMENTAL DETAILS

The experimental apparatus and the procedure used in the present work have been described in detail elsewhere.[20] Briefly, the experiments were conducted in a home-built ultrahigh vacuum system with a base pressure better than 1×10^{-10} Torr. Unless stated otherwise, all of the EELS measurements were conducted using a custom-built EELS spectrometer described previously,[20] with the sample held at room temperature in a specular reflection scattering geometry at 45° from the surface normal. A routine energy resolution of 20 meV (or 160 cm^{-1}) full width at half maximum with a typical count rate of 50 000 counts/s for the elastic peak could be obtained with our spectrometer operating at an impact energy of 5 eV. It should be noted that the calibration and tuning of the EELS spectrometer typically limited the reproducibility of the measured peak positions to 2 meV (or 16 cm^{-1}) in the present work.

A p-type, boron-doped Si(111) wafer (0.5 mm thick) with a resistivity of 40 Ω cm and a stated purity of 99.999% was purchased from Virginia Semiconductor Inc. A 8×6 mm^2 Si(111) sample was mechanically fastened to a Ta sample plate with 0.25-mm-diameter Ta wires, and it could be annealed by electron bombardment from a heated tungsten filament at the backside. The Si(111) sample was cleaned by a standard procedure involving repeated cycles of Ar^+ sputtering (1.5 kV, 4.2 $\mu A/cm^2$) for 30 min and annealing to 1200 K until a sharp (7×7) low-energy electron diffraction (LEED) pattern was observed. The cleanliness of the 7×7 surface was further verified *in situ* by the lack of any detectable vibrational EELS feature attributable to surface contamination from the ambient, particularly the Si—C stretching mode commonly found at 800–850 cm^{-1}. Glacial acetic acid (99.7% purity, Baker) was used without further purification, after appropriate degassing by repeated freeze-pump-thaw cycles. Exposure of acetic acid vapors to a clean Si(111) sample was performed at room temperature by backfilling the chamber at a typical pressure of 1×10^{-7} Torr using an uncalibrated variable leak valve. Unless stated otherwise, a saturation exposure (100 L, 1 Langmuir=1 $\times10^{-6}$ Torr s) of acetic acid was used for the present study, and the corresponding (7×7) LEED pattern of the clean surface was replaced with a diffuse (1×1) pattern.

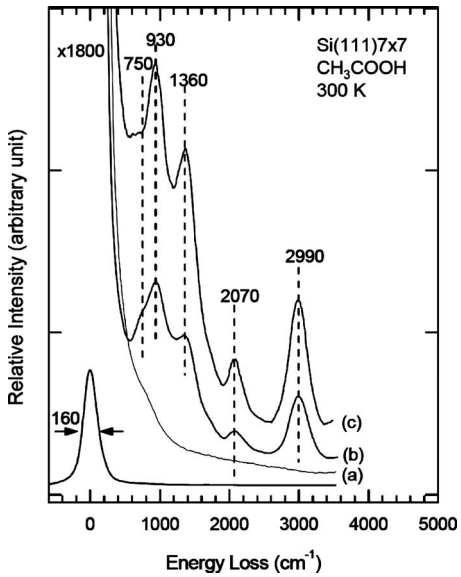

FIG. 1. Vibrational electron energy loss spectra for (a) a clean Si(111)7×7 surface and for 100 L acetic acid exposed to (b) clean Si(111)7×7, and (c) sputtered Si(111)7×7 at room temperature.

III. RESULTS AND DISCUSSION

A. Adsorption at room temperature

Figure 1 compares the EELS spectra of a 100 L exposure of acetic acid to a clean 7×7 and a sputtered Si(111)7×7 surface at room temperature. Evidently, the EELS spectrum for the saturation exposure to the clean 7×7 surface [Fig. 1(b)] exhibits several features at 750, 930, 1360, 2070, and 2990 cm^{-1}, respectively. The weak feature at 750 cm^{-1}, appearing as a shoulder of the feature at 930 cm^{-1}, is attributed to the Si—O stretching mode, ν(Si—O), based on earlier EELS studies on Si(111) surfaces exposed to H_2O [ν(Si—O)=766 cm^{-1}],[21] CH_3OH [ν(Si—O)=782 cm^{-1}],[22] and HCOOH [ν(Si—O)=710 cm^{-1}].[17] The feature at 2070 cm^{-1} is assigned to the Si—H stretching mode, ν(Si—H), by reference to the EELS study of the Si(111)-H system [with ν(Si—H)=2080 cm^{-1}].[23] By comparing with the vibrational modes of acetic acid chemisorbed on silica (producing CH_3COO—Si),[24] isolated methyl acetate molecules (CH_3COOCH_3, in the gas phase),[25] acetate ions in solution,[26] and isolated acetic acid molecules (as monomers in the gas phase),[27] the remaining features at 930, 1360, and 2990 cm^{-1} can be attributed to the C—C stretching mode, ν(C—C), CH_3 symmetric deformation mode, $\delta_s(CH_3)$, and CH_3 stretching mode, $\nu(CH_3)$, respectively. The C—O stretching mode, ν(C—O), and the C═O stretching mode, ν(C═O), observed at 1264 and 1788 cm^{-1}, respectively, for

isolated acetic acid molecules are not easily discernible in Fig. 1, which suggests that these bonds are either absent or oriented nearly parallel to the surface. Similarly, the C=O stretching mode has been reported at 1765 cm^{-1} for the surface CH_3COO—Si adspecies,[24] where Si is a surface silicon atom of silica. Table I summarizes our assignments of the observed EELS features of acetic acid on Si(111)7×7, with reference to the reported assignments for CH_3COO—Si,[24] CH_3COOCH_3,[25] acetate ions in solution,[26] and isolated acetic acid molecules,[27] as well as chemisorbed acetic acid on Ge(100)2×1 (on which both unidentate and bidentate acetates were observed).[14] The presence of the ν(Si—H) feature at 2070 cm^{-1} suggests O—H dissociative adsorption of acetic acid on Si(111)7×7, while that of the ν(Si—O) feature at 750 cm^{-1} indicates the attachment of the acetate adspecies to the Si surface through the formation of a Si—O bond. The lack of well-resolved EELS features that can be clearly attributed to C—O and C=O stretching modes as expected for unidentate adstructures, and/or to O···C···O symmetric and asymmetric stretching modes for bidentate adstructures makes it difficult to unambiguously identify the adsorption geometry of the acetate. The strong intensity of the observed ν(C—C) feature at 930 cm^{-1} indicates that the C—C bond is oriented nearly along the surface normal. This in turn suggests that any adstructure, in either unidentate or bidentate configuration, would have the C—O and C=O bonds oriented near-parallel to the surface, making the corresponding vibrational features inherently weak (in accord with the surface selection rule) and difficult to detect.

In order to clarify the plausible adstructures, we performed DFT calculations using the GAUSSIAN03 package.[28] Since a diffuse (1×1) LEED pattern was observed for a saturation exposure of acetic acid on Si(111)7×7, DFT calculations were carried out for dissociative adsorption of acetic acid on reconstructed 7×7 and unreconstructed 1×1 model surfaces of Si(111) expected at low and high exposures, respectively. Given the large number of possible adsorption sites on the 7×7 surface, we have chosen only the sites corresponding to the more abundant adatom-restatom pair. A $Si_{16}H_{18}$ cluster was used to represent the restatom-adatom sites at the faulted half of the Si(111)7×7 unit cell, after adopting the dimer-adatom-stacking fault model of Takayanagi *et al.*[16] With additional third and fourth Si sublayers, the present larger $Si_{16}H_{18}$ cluster should be more reliable than the smaller Si_9H_{12} cluster commonly used to model the 7×7 surface. The employed hybrid density functional B3LYP consisted of Becke's three-parameter nonlocal-exchange functional[29] and the correlation functional of Lee–Yang–Parr.[30] Three standard 6–31G(d), 6-31+G(d), and 6-31++G(d,p) basis sets[28] have been used, and all gave similar results for the optimized geometries and total energies (with the larger basis set generally providing a lower total energy). The separation between the adatom and restatom in the free $Si_{16}H_{18}$ cluster has been constrained to the experimental value (4.57 Å).[16] The corresponding adsorption energy (for acetic acid), ΔE, was estimated by the difference between the total energy for the optimized structure of an unidentate adsorbate-substrate configuration (ASC) of the acetic acid adsorbate on the $Si_{16}H_{18}$ model surface and the sum of the total energies of a free acetic acid molecule and of the $Si_{16}H_{18}$ cluster. In the case of the bidentate ASC, two independent $Si_{16}H_{18}$ clusters were used to separately accommodate bonding with the bidentate acetate and the dissociated H atom. The corresponding ΔE was then estimated by the difference between the sum of the total energies for the bidentate ASC on a $Si_{16}H_{18}$ cluster and for a H atom on a second $Si_{16}H_{18}$ cluster optimized separately and the sum of the total energies of a free acetic acid molecule and of two independent (identical) $Si_{16}H_{18}$ clusters. All the total energies were obtained without zero-point correction, and no correction to the basis set superposition error was made to ΔE. We then repeated the calculations using a $Si_{16}H_{22}$ cluster to simulate a model Si(111)1×1 surface. The resulting calculated adstructure geometries, adsorption energies, and vibrational wavenumbers are all found to be similar to those found for the respective unidentate and bidentate cases on the model 7×7 surface. It should be noted that geometry optimizations for the ASCs are obtained without fixing the atom positions in the clusters and the adsorbates. As summarized in Table I, the largest differences in the wavenumbers for unidentate ASCs on the 7×7 and 1×1 model surfaces are found in the C=O stretch (26 cm^{-1}) and C—O stretch (25 cm^{-1}), followed by those in the Si—O stretch (13 cm^{-1}) and C—C stretch (12 cm^{-1}). The differences in the wavenumbers for the remaining vibrations are less than 7 cm^{-1}. In the case of the respective bidentate ASCs, the corresponding largest wavenumber differences are found in the OCO asymmetric stretch (20 cm^{-1}) and C—C stretch (15 cm^{-1}).

Figure 2 shows two plausible adstructures on the model $Si_{16}H_{18}$ surface [simulating part of the Si(111)7×7] arising from O—H dissociation obtained by DFT/B3LYP calculation with the 6–31G(d) basis set. In particular, ASC A [Fig. 2(a)] corresponds to unidentate acetate and dissociated H atom on the adatom and restatom sites, respectively, and vice versa for ASC B [Fig. 2(b)]. Evidently, ASC A, with the adsorption energy ΔE=−271.4 kJ mol^{-1}, is slightly more stable than ASC B, with ΔE=−262.8 kJ mol^{-1}. Given the small difference in ΔE between ASCs A and B and their structural similarities, the slightly less stable ASC B cannot be ruled out at room temperature based on energetics consideration alone. However, the electron-rich acetate fragment would tend to bond with electron-deficient Si adatom site (instead of electron-rich Si restatom). We therefore expect ASC A would be the naturally preferred adstructure. For O—H dissociative adsorption of acetic acid on the 7×7 surface, the calculated wavenumbers of the respective vibrational modes for both unidentate ASCs A and B are nearly the same, with the values for ASC B generally within 24 cm^{-1} higher than the corresponding ASC A values for all vibrations except the ν(C=O) mode. Given the lower total energy, ASC A appears to be the more likely adsorption arrangement. However, these differences between ASC A and ASC B are small, and therefore the presence of a minor population of ASC B cannot be ruled out. Figure 2(c) shows the bidentate ASC C, with a more tilted bonding orientation from the surface normal than those found for the unidentate ASCs A and B, which could give rise to a weaker ν(C—C)

TABLE I. Comparison of experimental vibrational wavenumbers (in cm^{-1}) for acetic acid chemisorbed on Si(111)7×7 with experimental data for acetic acid on silica ($CH_3COO—Si$) (Ref. 24), isolated methyl acetate (CH_3COOCH_3) molecules (Ref. 25), acetate ions in solution (Ref. 26), isolated acetic acid molecules in the gas phase (Ref. 27), and acetic acid chemisorbed on Ge(100)2×1 (Ref. 14), and with calculated wavenumbers for unidentate and bidentate ASCs on model Si(11)7×7 and Si(111)1×1 surfaces obtained by B3LYP/6–31G(d) DFT calculations.

							B3LYP/6–31(d) DFT calculations (this work)					
Vibrational mode (cm^{-1})	Acetic acid on Si(111)7×7 (this work)	Acetic acid on silica (Ref. 24)	Methyl acetate (Ref. 25)	Acetate ions in solution (Ref. 26)	Acetic acid monomer (Ref. 27)	Acetic acid on Ge(100) 2×1 (Ref. 14)	Acetic acid monomer	Unidentate ASC A on Si(111)7×7	Unidentate ASC B on Si(111)7×7	Bidentate ASC C on Si(111)7×7	Unidentate ASC D on Si(111)1×1	Bidentate ASC E on Si(111)1×1
δ(OCO)	⋯	⋯	⋯	650	642	⋯	582	⋯	⋯	634, 677	⋯	634, 676
ν(Si—O)	750	⋯	⋯	⋯	⋯	⋯	⋯	761–778	770	792	757	788
ν(C—C)	930	⋯	844	926	847	⋯	866	928	947	935, 947	934	938, 962
$\rho(CH_3)$	⋯	⋯	980	1052	1048	⋯	1080	1032	1039	1077	1036	1077
ν(C—O)	⋯	⋯	1248	⋯	1264	1267	1225	1259	1283	993, 947	1284	1001, 962
$\delta_s(CH_3)$	1360	1377	1375	1344	1382	1364	1434	1423	1423	1433	1423	1433
$\delta_{as}(CH_3)$	⋯	1439	1430	⋯	1430	⋯	1501	1498	1498	1502	1497	1502
ν_s(OCO)	⋯	⋯	⋯	1413	⋯	1433	⋯	⋯	⋯	1249	⋯	1258
ν_{as}(OCO)	⋯	⋯	⋯	1556	⋯	1458	⋯	⋯	⋯	1167	⋯	1187
ν(C═O)	⋯	1765	1771	⋯	1788	1674	1858	1809	1796	⋯	1783	⋯
ν(Si—H)	2070	⋯	⋯	⋯	⋯	1971[a]	⋯	2236	2239	2190, 2204[b]	2236	2190, 2203[b]
$\nu_s(CH_3)$	2990[c]	2951	2964	2935	2944	⋯	3073	3073	3073	3007	3073	3003
$\nu_{as}(CH_3)$	2990[c]	2996	3031	⋯	2996	⋯	3134	3135	3135	3108	3135	3109
$\nu'_{as}(CH_3)$	⋯	⋯	⋯	⋯	⋯	⋯	⋯	3185	3185	3153	3185	3154
ν(O—H)		⋯	⋯	⋯	3583	⋯	3687	⋯	⋯	⋯	⋯	⋯

[a] ν(Ge—H) gives the corresponding stretching mode of Ge—H.
[b] It should be noted that the Si—H stretching modes were calculated for a dissociated H atom on a separate cluster ($Si_{16}H_{18}$ for ASC C and $Si_{18}H_{22}$ for ASC E). The smaller and larger wavenumbers correspond to H adsorption on a restatom and an adatom, respectively.
[c] Unresolved features in experiment.

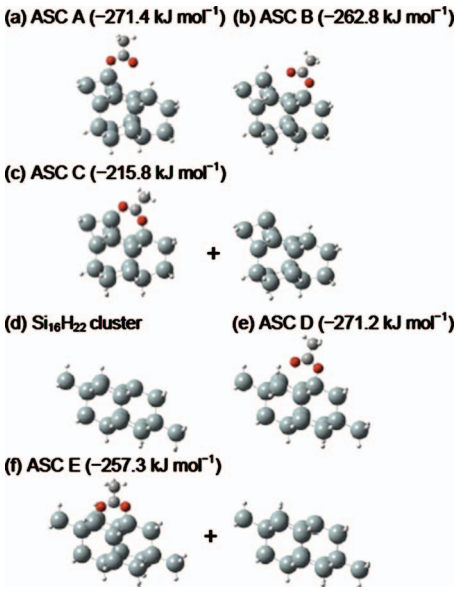

FIG. 2. Optimized geometries and adsorption energies (in parentheses) of ASCs of [(a) and (b)] unidentate acetate and (c) bidentate acetate for dissociative adsorption of acetic acid over an adatom-restatom site on the surface of a $Si_{16}H_{18}$ cluster, and of (d) a $Si_{16}H_{22}$ cluster with all but two of the Si atoms terminated with H atoms, (e) unidentate acetate and (f) bidentate acetate for dissociative adsorption of acetic acid on the $Si_{16}H_{22}$ cluster. All the calculations were obtained by DFT B3LYP/6–31G(d).

feature. Furthermore, the new features involving the OCO moiety at 634, 677, 1167, and 1249 cm^{-1} found for ASC C (Table I) could potentially be used to uniquely identify the presence of this bidentate ASC. However, these intensity differences and new features are not easily distinguishable from the unidentate features. Given the considerably higher ΔE calculated for ASC C (−215.8 kJ mol^{-1}) than those for the unidentate ASCs (−271.4, −262.8 kJ mol^{-1}) and the discernibly shorter adatom-restatom separation for ASC C (~3.7 Å, cf. ~4.5 Å for ASCs A and B, and for the pristine 7×7 surface determined experimentally), the presence of bidentate ASC is less probable based on energy or structure consideration.

Figure 2 also shows two plausible adstructures on the model $Si_{16}H_{22}$ surface (simulating the unreconstructed Si(111)1×1 surface) arising from O—H dissociation obtained by DFT/B3LYP calculation with the 6–31G(d) basis set. In particular, ASC D [Fig. 2(e)] corresponds to unidentate acetate and dissociated H atom on Si(111)1×1 with the adsorption energy $\Delta E = -271.2$ kJ mol^{-1}. As shown in Table I, the calculated wavenumbers for different vibrational modes for ASC D are in good accord with our EELS data, with differences of less than 63 cm^{-1} from the observed ν(Si—O) at 750 cm^{-1}, ν(C—C) at 930 cm^{-1}, and $\delta_s(CH_3)$ at 1360 cm^{-1} and of less than 166 cm^{-1} from the observed ν(Si—H) at 2070 cm^{-1}, and $\nu_s(CH_3)$ at 2990 cm^{-1}. It should be noted that the calculated wavenumbers have not been multiplied by any correction factor as commonly practiced for condensed materials in the literature. The ν(C—O) and ν(C=O) wavenumbers for ASC D are 1284 and 1783 cm^{-1}, respectively, which do not correspond to any well-resolved EELS feature in Fig. 1. This is not surprising because the C—O and C=O bonds are nearly parallel to the surface, which would lead to rather weak perpendicular dipole-moment component. Figure 2(f) shows the bidentate ASC E, with a more tilted bonding orientation from the surface normal than those found for the unidentate ASC D [Fig. 2(e)], which could give rise to a weaker ν(C—C) feature. Similar to that observed for the unidentate [Figs. 2(a) and 2(b)] and bidentate ASCs for the model 7×7 surface [Fig. 2(c)], the new features involving the (more surface parallel) OCO moiety at 634, 676, 1187, and 1258 cm^{-1} found for ASC E (Table I) are weak and are not easily distinguishable from the unidentate features. Similarly, given the higher ΔE calculated for ASC E (−257.3 kJ mol^{-1}) than those for the unidentate ASC D (−271.2 kJ mol^{-1}) and the notably shorter Si—O separation in the bidentate ASC E (3.4 Å) than those for $Si_{16}H_{22}$ (3.9 Å) and for the 1×1 surface (3.84 Å),[31] the presence of bidentate ASC E is therefore less likely.

The present DFT calculations therefore provide strong support for unidentate O—H dissociative adsorption of acetic acid on Si(111)7×7, which is in accord with other surface acetates found in the unidentate adsorption geometry for formic acid[17,18] and methacrylic acid[19] on Si(111)7×7. The adsorption of acetic acid on Si(100)2×1 (Ref. 8) and Ge(100)2×1 (Ref. 14) therefore proceeds similarly through O—H dissociation, with the surface acetate in both bidentate and unidentate geometries depending on the coverage. This similarity highlights the importance of the local bonding structure of the Si surface, and particularly the availability of directional dangling bonds as the key factor, in controlling the adsorption of a carboxylic acid on the Si surface.

Ion bombardment of a solid surface results in processes such as ion backscattering, sputtering of surface atoms, and ion implantation, all of which could generate new reactive sites and structural defects in the surface and subsurface region, depending on the range of the ions in the solid. In order to study the adsorption of acetic acid on possible local sites not restricted to those available on a single-crystal surface, the clean Si(111)7×7 substrate was bombarded with normally incident Ar^+ ions at 1.5 keV beam energy with a fluence of 4×10^{14} ions/cm^2 since such a sputtering condition is expected to result in both surface and bulk amorphization of Si(111)7×7.[32] Sputtering results in an increase in the full width at half maximum of the elastic peak from 160 to 200 cm^{-1}, indicating a decrease in the surface ordering. Figure 1(c) shows the EELS spectrum of 100 L acetic acid on a sputtered Si(111) surface at room temperature. With the exception of minor changes in the relative spectral intensity, the EELS spectrum for the sputtered sample [Fig. 1(c)] appears remarkably similar in shape and spectral locations to that for the 7×7 sample [Fig. 1(b)]. Similar assignments for these EELS features observed for the sputtered surface can therefore be made. When compared to the EELS spectrum for acetic acid adsorption on the 7×7 surface [Fig. 1(b)], the relative intensity of the ν(Si—O) feature at 750 cm^{-1} for acetic acid adsorption on the sputtered surface is reduced while the $\delta(CH_3)$ feature at 1360 cm^{-1} becomes more prominent, all with respect to the ν(C—C) feature at 930 cm^{-1} [Fig. 1(c)]. The reduction in the ν(Si—O) spectral intensity for the sputtered sample suggests that the unidentate acetate adspecies on the sputtered surface are, in contrast

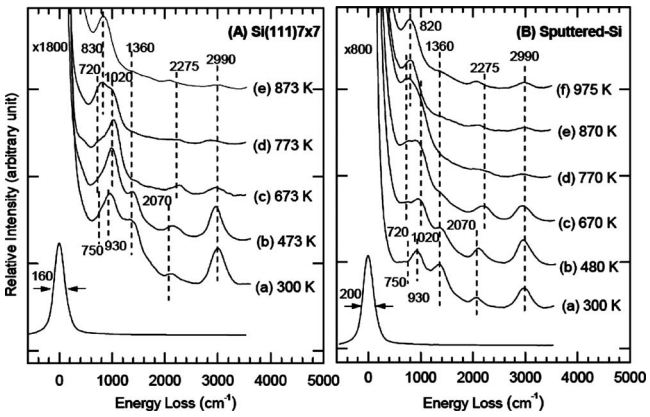

FIG. 3. Vibrational electron energy loss spectra for 100 L acetic acid exposed to (A) clean Si(111)7×7 and (B) sputtered Si(111)7×7 at room temperature, and upon sequential flash-annealing to (b) 473–480 K, (c) 670–673 K, (d) 770–773 K, (e) 870–873 K, and (f) 975 K.

to the 7×7 case, no longer necessary to orient near-perpendicular to the surface, which in turn reduces the corresponding dipole moment. The observed formation of unidentate acetate through O—H dissociative adsorption of acetic acid on the sputtered Si surface therefore confirms that the local bonding sites are more important in driving the dissociative adsorption process.

B. Thermal evolution of surface acetate

Figure 3(A) shows the EELS spectra of 100 L room-temperature exposure of acetic acid on Si(111)7×7 upon successive flash-annealing to different temperatures (and cooled back to room temperature before collecting the EELS spectra). Evidently, annealing the sample to 473 K (Fig. 3(A)b) appears to reduce the $\delta(CH_3)$ feature at 1360 cm^{-1} and the $\nu(CH_3)$ feature at 2990 cm^{-1} slightly, with subtle changes to the other spectral features at lower wavenumbers. In particular, the weak ν(Si—O) feature at 750 cm^{-1} becomes indistinct and replaced by new features at 720 and 1020 cm^{-1} that could be attributed to, respectively, the rocking and asymmetric stretching modes of Si—O—Si species.[33] This change marks the onset of the C—O bond cleavage in the surface acetate and the incorporation of the dissociated O atoms into the Si surface. Upon further annealing to 673 K [Fig. 3(A)c], the new Si—O—Si features at 720 and 1020 cm^{-1} become more evident, while the intensities of the CH_3 features at 1360 and 2990 cm^{-1} and of the ν(C—C) feature at 930 cm^{-1} are found to decrease considerably. These latter changes suggest thermal desorption of the dissociated C- and O-containing fragments. In particular, given the average bond dissociation energies (in kJ mol^{-1}) for Si—O (460), C—O (358), C=O (749), C—C (347), C—H (414), Si—H (314), and O—H (465),[34] the C—C and C—O bonds (along with the Si—H bond) are the weakest, which suggests that the likely dissociated fragments are CH_3, C=O, and O atoms on the 7×7 surface. The ν(Si—H) feature observed at 2070 cm^{-1} at room temperature has undergone a shift to 2275 cm^{-1} after flash annealing to 673 K, which suggests the formation of multihydrides with the SiH_2 and SiH_3 stretching modes on Si(111) reported at 2112 and 2145 cm^{-1}, respectively.[21,35] The latter Si—H feature at 2275 cm^{-1} becomes totally diminished upon further annealing to 773 K, which is consistent with the recombinative H_2 desorption for Si hydrides found near this temperature.[36] Further flash annealing the sample to 773 K [Fig. 3(A)d] also strengthens the Si—O—Si features at 720 and 1020 cm^{-1}, and it produces a new feature at 830 cm^{-1} that is attributed to the Si—C stretching mode, which suggests that the remaining surface species (dissociated CH_3CO fragments) has undergone C—C bond scission, producing dissociated C atoms that react with the Si atoms to form the surface SiC species. These observations are analogous to that found for formic acid on Si(111),[37] for which the formate species decomposes to form predominantly the Si—O—Si and SiC species on Si(111) upon heating to 550 K. Flash-annealing to 873 K [Fig. 3(A)e] completely removes all the EELS features, leaving the single ν(Si—C) peak at 830 cm^{-1}, consistent with the presence of the SiC products at this high temperature after total desorption of the remaining thermally decomposed species.

As shown in Fig. 3(B), similar spectral evolution with respect to flash-annealing can also be found in the EELS features for 100 L acetic acid on the sputtered Si(111) surface. In particular, upon flash-annealing the sputtered sample to 670 K [Fig. 3(B)c], the ν(Si—O) feature at 750 cm^{-1} is gradually replaced by the rocking mode at 720 cm^{-1} and asymmetric stretching mode at 1020 cm^{-1} of the Si—O—Si species, and the ν(Si—H) at 2070 cm^{-1} is shifted to 2275 cm^{-1}, while the $\nu(CH_3)$ feature at 1360 cm^{-1} and $\delta(CH_3)$ feature at 2990 cm^{-1} undergo graduate reduction in intensity, which indicates the formation of multihydrides attached to Si adatoms and the desorption of C- and O-containing fragments, respectively. Along with the blueshifted ν(Si—H) feature at 2275 cm^{-1}, these Si—O—Si and CH_3 features appear to greatly diminish at flash-annealing temperature of 770 K [Fig. 3(B)d], which indicates the recombinative desorption of H_2 for silicon monohydrides and the decomposition of the remaining dissociated C- and O-containing fragments. Formation of SiC becomes evident upon further flash-annealing to 770 K [Fig. 3(B)d], and its characteristic ν(Si—C) feature at 820 cm^{-1} becomes the only prominent feature upon annealing to 975 K [Fig. 3(B)f]. At 975 K, the remaining surface O atoms are believed to either desorb or diffuse into the bulk. The spectral similarities in the thermal evolution between the 7×7 [Fig. 3(A)] and the sputtered samples [Fig. 3(B)] again indicate that the local bonding environment controls the energetics and therefore the thermal evolution of the adspecies.

IV. CONCLUDING REMARKS

Acetic acid is found to undergo O—H dissociative adsorption on Si(111)7×7 at room temperature, producing an acetate adspecies, likely unidentately bonded to the silicon surface through the formation of a Si—O bond. The equilibrium structures and the corresponding vibrational wavenumbers obtained from the DFT calculations are consistent with the vibrational EELS data. Subsequent flash-annealing the sample causes interesting spectral changes, providing

subtle clues to the thermal breakdown of the acetate adspecies. In particular, the onset of C—O dissociation and the formation of Si—O—Si species at 473 K, and the reduction of C—C and CH_3 fragments at 673 K are found to be followed by reduction of the Si monohydrides (likely as recombinatively desorbed H_2) at 773 K, and the formation of SiC as the only remaining adproduct at 873 K. Both the room-temperature adsorption and thermal evolution of the surface species on a sputtered Si surface are similar to those observed for Si(111)7×7, suggesting the adsorption and thermal chemistry occurring largely at local sites.

ACKNOWLEDGMENTS

This work was supported by the Natural Sciences and Engineering Research Council of Canada. We thank Dr. M. M. Thiam for useful suggestions and discussions.

[1] F. Cattaruzza, A. Cricenti, A. Flamini, M. Girasole, G. Longo, A. Mezzi, and T. Prosperi, J. Mater. Chem. **14**, 1461 (2004).
[2] M. Perring, S. Dutta, S. Arafat, M. Mitchell, P. J. A. Kenis, and N. B. Bowden, Langmuir **21**, 10537 (2005).
[3] A. Lopez, T. Heller, T. Bitzer, and N. V. Richardson, Chem. Phys. **277**, 1 (2002).
[4] A. Lopez, Q. Chen, and N. V. Richardson, Surf. Interface Anal. **33**, 441 (2002).
[5] J. Y. Huang, Y. S. Ning, K. S. Yong, Y. H. Cai, H. H. Tang, Y. X. Shao, S. F. Alshahateet, Y. M. Sun, and G. Q. Xu, Langmuir **23**, 6218 (2007).
[6] T. R. Lefwich and A. V. Teplyakov, Surf. Sci. Rep. **63**, 1 (2008).
[7] H. Asanuma, G. P. Lopinski, and H. Z. Yu, Langmuir **21**, 5013 (2005).
[8] M. Ebrahimi, J. F. Rios, and K. T. Leung, J. Phys. Chem. C **113**, 281 (2009).
[9] H. K. Lee, K. Kim, J. Han, T. H. Kang, J. W. Chung, and B. Kim, Phys. Rev. B **77**, 115324 (2008).
[10] H. J. Kim and J. H. Cho, Phys. Rev. B **72**, 195305 (2005).
[11] M. Carbone and R. Caminiti, Surf. Sci. **602**, 852 (2008).
[12] H. J. Kim and J. H. Cho, J. Phys. Chem. C **112**, 6947 (2008).
[13] E. Hwang, D. H. Kim, Y. J. Hwang, A. Kim, S. Hong, and S. Kim, J. Phys. Chem. C **111**, 5941 (2007).
[14] M. A. Filler, J. A. Van Deventer, A. J. Keung, and S. F. Bent, J. Am. Chem. Soc. **128**, 770 (2006).
[15] D. H. Kim, E. Hwang, S. Hong, and S. Kim, Surf. Sci. **600**, 3629 (2006).
[16] K. Takayanagi, T. Tanishiro, S. Takahashi, and M. Takahashi, J. Vac. Sci. Technol. A **3**, 1502 (1985).
[17] S. Tanaka, M. Onchi, and M. Nishijima, Chem. Phys. Lett. **146**, 67 (1988).
[18] J. Y. Huang, H. G. Huang, K. Y. Lin, Q. P. Liu, Y. M. Sun, and G. Q. Xu, Surf. Sci. **549**, 255 (2004).
[19] J. Y. Huang, Y. X. Shao, H. G. Huang, Y. H. Cai, Y. Sheng Ning, H. H. Tang, Q. P. Liu, S. F. Alshahateet, Y. M. Sun, and G. Q. Xu, J. Phys. Chem. B **109**, 19831 (2005).
[20] D. Hu, Ph.D. thesis, University of Waterloo, 1993.
[21] M. Nishijima, K. Edamoto, Y. Kubota, S. Tanaka, and M. Onchi, J. Chem. Phys. **84**, 6458 (1986).
[22] K. Edamoto, Y. Kubota, M. Onchi, and M. Nishijima, Surf. Sci. **146**, L533 (1984).
[23] H. Kobayashi, K. Edamoto, M. Onchi, and M. Nishijima, J. Chem. Phys. **78**, 7429 (1983).
[24] R. P. Young, Can. J. Chem. **47**, 2237 (1969).
[25] T. Shimanouchi, *Tables of Molecular Vibrational Frequencies Consolidated* (National Bureau of Standards, Washington, DC, 1972), Vol. I, pp. 1–160.
[26] K. Ito and H. J. Bernstein, Can. J. Chem. **34**, 170 (1956).
[27] M. Haurie and A. Novak, J. Chim. Phys. Phys.-Chim. Biol. **62**, 137 (1965).
[28] M. J. Frisch, G. W. Trucks, H. B. Schlegel *et al.*, GAUSSIAN03, Revision A.1, Gaussian, Inc., Pittsburgh PA, 2003.
[29] A. D. Becke, J. Chem. Phys. **98**, 5648 (1993).
[30] C. Lee, W. Yang, and R. G. Parr, Phys. Rev. B **37**, 785 (1988).
[31] D. G. Zhao, S. J. Xu, M. H. Xie, and S. Y. Tong, Appl. Phys. Lett. **83**, 677 (2003).
[32] W. Bock, H. Gnaser, and H. Oechsner, Surf. Sci. **282**, 333 (1993).
[33] H. Ibach, H. D. Bruchmann, and H. Wagner, Appl. Phys. A: Mater. Sci. Process. **29**, 113 (1982).
[34] R. T. Sanderson, *Chemical Bonds and Bond Energy* (Academic, New York, 1976).
[35] M. Niwano, M. Terashi, and J. Kuge, Surf. Sci. **420**, 6 (1999).
[36] K. Oura, V. G. Lifshits, A. A. Saranin, A. V. Zotov, and M. Katayama, Surf. Sci. Rep. **35**, 1 (1999).
[37] S. Tanaka, M. Onchi, and M. Nishijima, J. Chem. Phys. **91**, 2712 (1989).